PHYSICAL REVIEW B **85**, 121404(R) (2012)

Electron localization in epitaxial graphene on Ru(0001) determined by moiré corrugation

D. Stradi,[1,2] S. Barja,[2,3] C. Díaz,[1] M. Garnica,[2,3] B. Borca,[3] J. J. Hinarejos,[3] D. Sánchez-Portal,[4,5] M. Alcamí,[1] A. Arnau,[4,5,6] A. L. Vázquez de Parga,[2,3] R. Miranda,[2,3] and F. Martín[1,2,*]

[1]*Departamento de Química, Módulo 13, Universidad Autónoma de Madrid, 28049 Madrid, Spain*
[2]*Instituto Madrileño de Estudios Avanzados en Nanociencia (IMDEA-Nanociencia), Cantoblanco, 28049 Madrid, Spain*
[3]*Departamento Física de la Materia Condensada, Universidad Autónoma de Madrid, 28049 Madrid, Spain*
[4]*Materials Physics Center (CSIC-UPV/EHU), Paseo Manuel de Lardizábal 5, 20018 San Sebastián, Spain*
[5]*Donostia International Physics Centre (DIPC), Paseo Manuel de Lardizábal 4, 20018 San Sebastian, Spain*
[6]*Departamento Física de Materiales (UPV/EHU), Facultad de Química, Apartado 1072, 20080 San Sebastián, Spain*

(Received 21 November 2011; revised manuscript received 3 February 2012; published 14 March 2012)

The interpretation of scanning tunneling spectroscopy (STS) and scanning tunneling microscopy measurements of epitaxial graphene on lattice-mismatched substrates is a challenging problem, because of the spatial modulation in the electronic structure imposed by the formation of a moiré pattern. Here we describe the electronic structure of graphene adsorbed on Ru(0001) by means of density functional theory calculations that include van der Waals interactions and are performed on a large 11×11 unit cell to account for the observed moiré patterns. Our results show the existence of localized electronic states in the high and low areas of the moiré at energies close to and well above the Fermi level, respectively. Localization is due to the spatial modulation of the graphene-Ru(0001) interaction and is at the origin of the various peaks observed in STS spectra.

DOI: 10.1103/PhysRevB.85.121404 PACS number(s): 73.20.−r, 68.37.Ef, 68.55.−a, 73.22.Pr

Spatially resolved scanning tunneling spectroscopy (STS) is widely used to characterize the electronic structure of complex adsorbates on surfaces[1–4] and, in particular, of graphene adsorbed on semiconductor[5–9] and metal[10–17] substrates. The interest for the latter is twofold. From a fundamental point of view, the details of the graphene-substrate interaction are important to understand the physics of graphite intercalated with metallic atoms.[18] From a more applied perspective, the recent demonstration of large-scale production of graphene sheets of ∼1 inch size by using copper as a substrate[19] could be important for industrial applications or to understand the physics of the graphene-metal interfaces present in the contacts of hypothetical graphene devices.[20]

Recent experimental work has shown that, when the graphene-substrate interaction is weak (i.e., it is almost exclusively due to van der Waals dispersions forces) as in graphene/Ir(111),[21,22] the graphene layer remains almost flat and its electronic structure is almost unaltered. In contrast, when covalent bonds mediate the graphene-substrate interaction, as in graphene/Ru(0001) (G/Ru for short), a highly corrugated moiré pattern is formed as a result of the mismatch between the graphene and substrate lattice constants.[23–25] Although van der Waals forces tend to compensate the consequences of this mismatch, recent density functional theory calculations including dispersion forces (DFT-D2) still predict a corrugation of ∼1.2 Å.[25] Therefore, the corresponding electronic bands are expected to be significantly distorted with respect to those of flat graphene, as illustrated by the highly structured profiles of recently measured STS $dI(dZ)/dV$ spectra.[14–16,26]

As a consequence of the important distortions with respect to flat graphene, interpretation of STM and STS spectra measured on G/Ru is a formidable challenge. An example of this is the measurement of the apparent corrugation of the moiré pattern as a function of the bias voltage in the scanning tunneling microscopy (STM) images.[27] In an attempt to measure spatially resolved dI/dV spectra around the Fermi level, an asymmetry of the local density of states (LDOS) in the high and low areas of the moiré pattern was found.[10] In addition to this asymmetry, pronounced peaks in the dI/dV spectra around the Fermi level have been observed.[10,11,16,28] This was interpreted as resulting from the shift of the graphene's Dirac point induced by electron doping from the Ru substrate,[10] which favors the high areas of the moiré (see also Refs. 16 and 29). More recently, Gyamfi and co-workers[15] have obtained dI/dV spectra with even sharper features. In contrast with previous work, these authors attribute the pronounced peak appearing in the STS spectra near the Fermi level at low negative bias voltages to a d-like Ru bulk state. So far, to the best of our knowledge, no interpretation based on first-principles calculations has been proposed to explain the shape and intensity of the spectral features observed in the dI/dV data.

Another controversial issue is the interpretation of the STS data measured on G/Ru at high positive bias voltage. In this case, and to the best of our knowledge, all the experimental data published so far are identical, but contradictory arguments have been used to explain the structures observed in the STS spectra at high positive voltage.[14,26,30,31] Based on a simple theoretical model that makes use of 1×1 flat graphene, Borca *et al.*[31] have conjectured that the STS peak observed at +3 eV in the low areas of the moiré is due to an interface state. However, Zhang *et al.*[30] have assigned this peak to the lowest field emission resonance (FER). The former authors have also claimed that the interface state is responsible for the inversion of contrast observed in STM images above +2.6 eV,[27] but there is no proof that this is indeed the case.

In this Rapid Communication we show that a *realistic* theoretical description of the electronic structure of G/Ru reproduces the main features observed in STS $dI(dZ)/dV$ spectra. We find that these features are due to electron localization in (i) states of the high areas of the moiré close

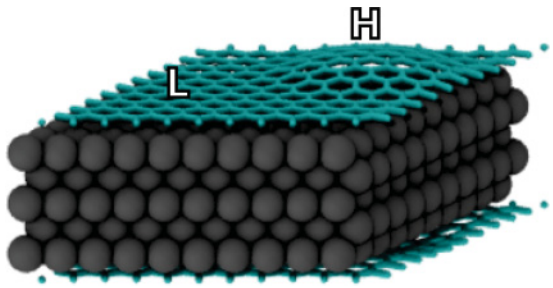

FIG. 1. (Color online) Structure of the symmetric $11 \times 11/10 \times 10$ G/Ru slab used in the calculations. Ru and C atoms are shown in dark gray and light blue (gray), respectively. H and L labels indicate the high and low areas of the graphene sheet.

to the Fermi level and (ii) unoccupied states of the low areas lying well above the Fermi level.

All calculations have been performed in the framework of DFT-D2 theory, which includes van der Waals interactions as described in Ref. 32. To model the G/Ru system, we have used a symmetric slab with five 10×10 Ru layers and two 11×11 graphene monolayers (see Fig. 1). The symmetric slab has been built by adding the mirror replica of the DFT-D2 optimized geometry obtained in Ref. 25 for a nonsymmetric slab with one 11×11 graphene monolayer lying on three 10×10 Ru layers (mirror placed at the topmost-2 Ru layer). The symmetry of the slab prevents spurious effects in the electronic density due to unphysical dipole contributions. By increasing the number of Ru layers to five, one can also expect a correct description of electronic states localized near the surface (see the Supplemental Material for the study of convergence with the number of Ru layers[33]). The electronic structure calculations have been performed with the VASP code,[34] by using the Perdew-Burke-Ernzerhof (PBE)[35] generalized gradient approximation (GGA) functional to describe the exchange-correlation energy. The projector augmented-wave (PAW) method[36] has been used to describe the ionic cores. The cutoff kinetic energy for the plane-wave expansion has been set to 400 eV, and the Brillouin zone has been sampled at the Γ point, using a Gaussian smearing of 0.1 eV. In order to avoid artifacts caused by the use of periodic boundary conditions in the direction perpendicular to the slab, a 20-Å vacuum layer has been placed between the slabs. STM simulated topographies and local density of states (LDOS) over selected areas of G/Ru have been computed by using the Tersoff-Hamann approximation.[37] The LDOS have been calculated as the average over a 30×30 LDOS grid on a 1×1 Ru(0001) unit-cell area, and the resulting spectra have been convoluted using a Gaussian function of 0.1-eV width, consistently with the thermal broadening of the electronic states used in the electronic structure calculations.

The experiments have been carried out in an ultrahigh vacuum (UHV) chamber with a base pressure of 4×10^{-11} Torr that contains a low-temperature STM and a rear-view low-energy electron diffraction (LEED) optics. The Ru(0001) crystal was cleaned by cycles of Ar^+ sputtering and annealing, followed by oxygen exposure and heating to high temperature.[38] The graphene layers were produced by thermal decomposition at 1200 K of ethylene molecules on the sample surface. The W tips were cleaned by ion bombardment and annealing in UHV to ensure a flat density of states at the tip apex.[39] The dI/dV curves were obtained by numerical differentiation of the $I(V)$ curves. For the $I(V)$ curves measured at high positive bias voltage we calculate instead the normalized differential tunneling conductance $[(dI/dV)/(I/V)]$ in order to reduce the exponential background and therefore improving the resolution.[40]

STS measurements [see Fig. 2(a), top panels] at low temperature (77 K) show that, close to the Fermi level, the spectra vary considerably with the position of the tip over the different regions of the graphene moiré: Spectra recorded over the high (H) regions show a well-defined series of peaks both at negative and positive bias voltages, while these structures are much less pronounced for spectra over the low (L) regions. In order to understand the origin of these features, we have computed the LDOS at different distances d from the Ru surface ($d = 0$ Å set at the Ru topmost layer). LDOS computed at $d = 7.43$ Å are shown in Fig. 2(a) (bottom panels). The choice of this value of d is compatible with the typical tip-surface distances in STS experiments.[41] We have checked that calculated LDOS remain qualitatively the same in the range $d \simeq 7$–8 Å [see the Supplemental Material for a detailed analysis of the variation of the LDOS with d (Ref. 33)]. At the H area of the moiré structure, where the coupling between the graphene monolayer and the metal substrate is weak, the LDOS shows two peaks at $E - E_F = -0.35$ eV and $E - E_F = +0.45$ eV.

At the L area [hcp/top site of the graphene moiré over Ru(0001)], the LDOS shows two small peaks at $E - E_F = -0.4$ eV and $E - E_F = +0.35$ eV [see Fig. 2(a), bottom left-hand panel]. Similar results have been obtained for the fcc/top site at the L area. These LDOS profiles qualitatively agree with those observed in the STS spectra. Nevertheless, at negative bias voltage, the measurements suggest the existence of two peaks instead of one at both the L and H areas. We will further elaborate on this particular issue below.

In order to get some insight on the origin of the observed peaks, we have integrated the density of states (DOS) in different energy ranges. Figure 2(b) shows two-dimensional (2D) cuts (xy plane) obtained after DOS integration, at 1 Å from the Ru(0001) surface (i.e., in between the graphene layer and the Ru surface). From Fig. 2(b) (left-hand column) it can be seen that if the DOS integration energy range includes a LDOS spectrum peak, a high electronic density is observed in the region right below the graphene ripple. On the contrary, accumulation of electronic density is barely seen if the integration energy range leaves out these LDOS peaks. To rule out that such an effect is due to the Ru surface reconstruction present on this system (see Fig. 1 of Ref. 25), we have integrated the DOS for the clean reconstructed Ru surface[42] [see Fig. 2(b), right-hand column]. The latter system does not exhibit localization of the electron density.

In Fig. 2(c), we compare the full spatial maps of the measured differential conductivity dI/dV with the integrated DOS shown in the lower left-hand panels of Fig. 2(b) at a similar bias voltage. The agreement is very good: Theory reproduces localization of the electron density in the H areas as well as the smaller contrast between H and L areas that is observed at positive bias voltage with respect to negative bias voltage. This reinforces the previous analysis and suggests

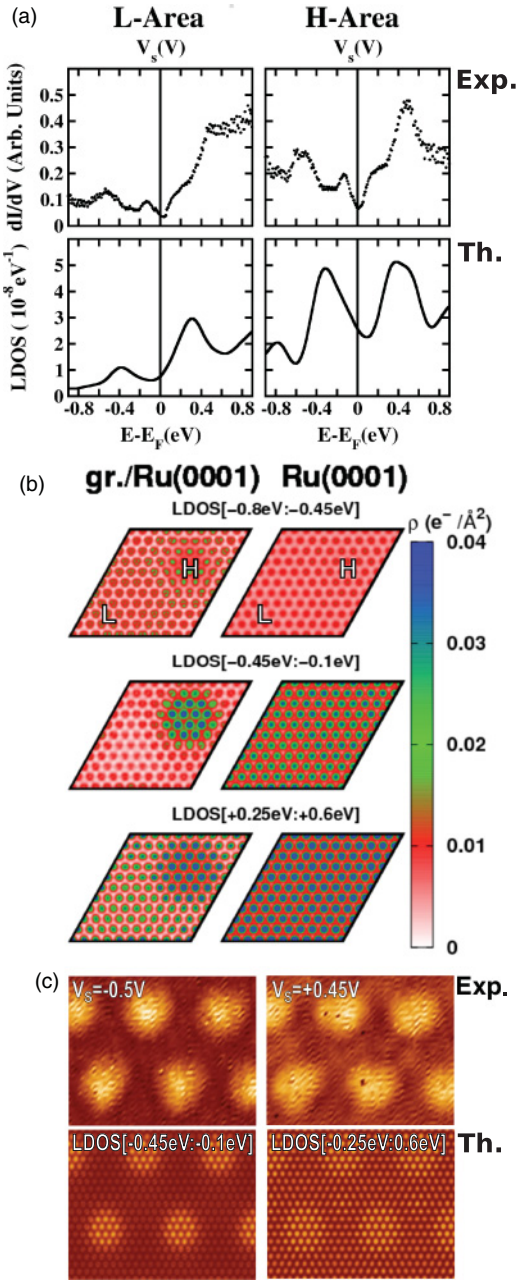

FIG. 2. (Color online) (a) Top: Experimental low-temperature STS near E_F, taken over the low region (left) and high region (right) of the graphene moiré. Bottom: Calculated LDOS at $d = 7.43$ Å over the Ru(0001) surface at the low area (left) and high area (right) of the graphene moiré. (b) xy cuts taken at ∼1 Å above the Ru(0001) topmost layer for selected integration ranges of the DOS, for G/Ru (left-hand column) and clean reconstructed Ru (right-hand column). (c) Experimental (top panels) dI/dV maps at the peak positions above and below E_F in the dI/dV spectra shown in (a), and corresponding xy cuts from (b). Individual $I(V)$ curves were measured at every pixel of the corresponding topographic image with a bias voltage of +1 V and a tunneling current of 0.4 nA. The dI/dV curves were obtained by numerical differentiation of the $I(V)$ curves.

that localization of electron density below the ripples is due to the formation of quantum dots. Less elaborate theoretical models[43,44] have also described spatial modulations of the electronic density of the graphene layer, but suggest[44] that localized states, if any, should only appear well below the Fermi level (∼−3.5 eV). Here we show that the localized states are clearly visible near the Fermi level, both below and above it.

To further check that the peaks observed in the H areas are indeed due to the presence of localized states, we have applied the stabilization method of Mandelshtam *et al.*[45,46] to a 1×1 unit-cell system formed by a layer of strained graphene lying pseudomorphically on n layers of Ru. Two values of the graphene-Ru(0001) distance, corresponding to those found in the H and L areas of corrugated graphene, have been used (H and L models for short). The number of Ru layers has been varied from $n = 3$ to 45 and the k sampling is $15 \times 15 \times 1$. In the H model, the density of resonant states (DORS) calculated in the K point unambiguously shows the existence of localized states at around −0.6 and +0.6 eV. In contrast, no such states are observed in the L model (see the Supplemental Material for more details[33]).

The small peak observed in the experimental spectra just below the Fermi level cannot be resolved in the full 11×11 calculations because these are performed with a too small number of k values and Ru layers. This small peak is also not seen in the DORS resulting from the H model. It is worth noticing that the integrated LDOSs shown in Fig. 2(b) for the 11×11 model resembles those of quantum dots described by a truncated triangular potential.[47] We have checked that this shape remains qualitatively the same when seven layers of Ru instead of five are used in the full 11×11 calculation.

In summary, the present results show that the peaks observed in STS near the Fermi level are due to the existence of localized electronic states in the high areas of the G/Ru moiré. This accumulation of electron density is due to electron doping from the Ru substrate in the H areas of the moiré.[10,29]

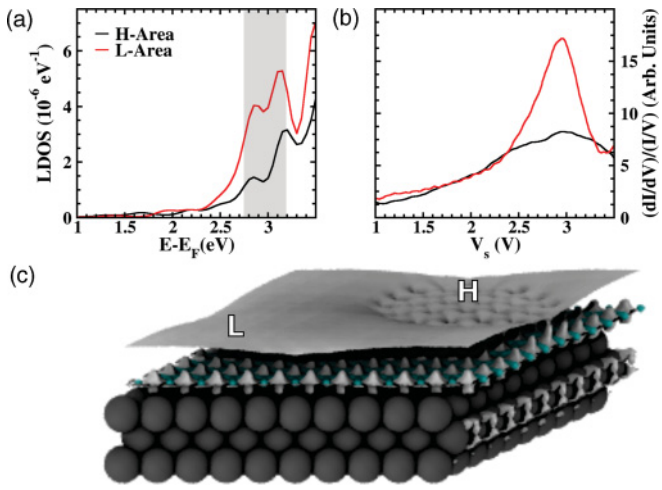

FIG. 3. (Color online) (a) LDOS taken at 7.43 Å above the Ru(0001) plane over the low (red/gray curve) and high (black curve) areas of the moiré. (b) STS spectra at high positive biases taken over the low (red/gray curve) and high (black curve) regions of the moiré. (c) Electronic density distribution obtained from the integration of the density of states (DOS) in the range between +2.75 and 3.2 eV [shaded area in (a)]. The color code is as in Fig. 1. Only three Ru layers are shown for simplicity.

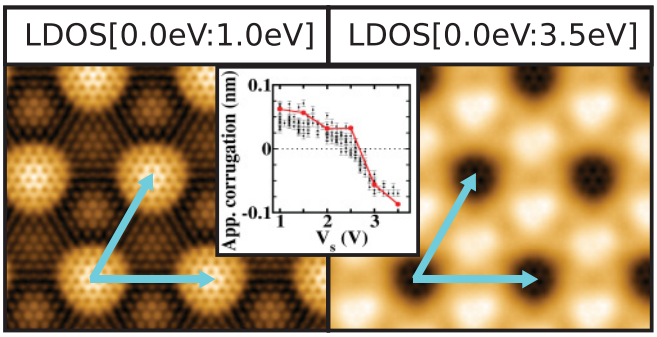

FIG. 4. (Color online) Simulated STM images for two different integration ranges of the LDOS, corresponding to $V_s = +1.0$ V (left) and $V_s = +3.5$ V (right). The STM images were calculated on an electron density contour of 1.69×10^{-4} Å^{-3} (see Ref. 25). To take into account the fact that electronic states contributing to the interfacial state are located above the graphene layer, the latter value has been multiplied by 10 when $V_s \geqslant 3$ eV. The inset shows the variation of the apparent corrugation with bias voltage (V_s). Black dots: Experimental results obtained with different experimental conditions (tip, tunneling current, samples, and temperature). Red (gray) dots: Theoretical results.

We now turn our attention to the unoccupied states probed at high bias voltages. STS experimental spectra [Fig. 3(b)] show an increase in dI/dV above 2.5 V for both H and L moiré areas, the increase being sharper for the L area. This experimental behavior is well reproduced by the theoretical LDOS at the same moiré areas and $d = 7.43$ Å [Fig. 3(a)].

An analysis of the electronic density distribution [Fig. 3(c)] obtained from integration of the DOS in the region where the LDOS exhibits its pronounced maximum (2.75–3.20 eV) shows that the origin of such a maximum is the protrusion of the electronic charge density outside the graphene layer exclusively in the L area of the moiré. We have identified the bottom of this interface band at the Γ point by a detailed analysis of the individual eigenstates: $E - E_F = 2.85$ eV.

This interfacial state, resulting from the hybridization of an unoccupied Ru(0001) surface resonance with the first image state component localized in the low areas of the moiré, was suggested[26] to be responsible for the inversion of contrast observed in G/Ru(0001) STM experiments at a bias voltage $V_s \sim +2.6$ V. To check this prediction and the accuracy of the present calculations, we have evaluated the apparent corrugation versus the applied bias voltage from $V_s = 0$ V up to $V_s = +3.5$ V. Figure 4 shows simulated STM images for two different integration ranges of the LDOS, corresponding to $V_s = +1.0$ V (left) and $V_s = +3.5$ V (right). The calculations reproduce the inversion of contrast observed in the experiments.[26] For completeness, the inset in Fig. 4 shows the variation of the apparent corrugation in the voltage range $V_s = +1.0$–3.5 eV. As can be seen, the theoretical results show negative apparent corrugation for voltage above the bottom of the interface band.

In summary, a realistic model for epitaxial monolayer graphene on Ru(0001) has allowed us to shed light on two controversial aspects regarding its electronic structure. We have shown that both the peaks appearing in STS spectra close to the Fermi level and the inversion of contrast observed in STM experiments are the result of the periodic modulation in the electronic properties induced by the formation of the moiré. The peaks observed close to the Fermi level in STS spectra recorded in the high regions of the moiré are due to the existence of localized electronic states in this region. At higher energies, the formation of an interface band strongly localized in the low regions of the moiré is responsible for the inversion of contrast observed in the STM topographies. Qualitatively speaking, the existence of localized states near the Fermi level is due to the opening of the graphene Dirac cone resulting from the interaction of graphene with the metal substrate. Thus, it is unlikely that such states are observed when the graphene-substrate interaction is weak, i.e., when graphene is barely corrugated. This is the reason why, in extended G/Ir(111), which is barely corrugated, localized electronic states are not seen. In the latter system, localized states can only be formed by building nanometer-size graphene islands on distant regions of the Ir substrate.[48–50] Recently, we became aware of results from a quite different experimental approach that also suggest the existence of quantum dots below the G/Ru ripples close to the Fermi level.[51]

We thank BSC-RES and CCC-UAM for allocation of computer time. Work supported by the MICINN Projects No. FIS2010-15127, No. FIS2010-18847, No. CTQ2010-17006, No. FIS-2010-19609-C09-00, No. ACI2008-0777, No. 2010C-07-25200, and No. CSD2007-00010, the CAM program NANOBIOMAGNET S2009/MAT1726, and the Gobierno Vasco-UPV/EHU Project No. IT-366-07. S.B. acknowledges financial support from MEC under FPU Grant No. AP-2007-00157.

*fernando.martin@uam.es

[1] J. Repp, G. Meyer, S. Paavilainen, F. E. Olsson, and M. Persson, Science **312**, 1196 (2006).
[2] P. Liljeroth, J. Repp, and G. Meyer, Science **317**, 1203 (2007).
[3] M. C. Lennartz, V. Caciuc, N. Atodiresei, S. Karthäuser, and S. Blügel, Phys. Rev. Lett. **105**, 066801 (2010).
[4] K. J. Franke, G. Schulze, and J. I. Pacual, Science **332**, 940 (2011).
[5] S. Y. Zhou, G.-H. Gweon, A. V. Fedorov, P. N. First, W. A. de Heer, D.-H. Lee, F. Guinea, A. H. Castro Neto, and A. Lanzara, Nat. Mater. **6**, 770 (2007).
[6] V. W. Brar, Y. Zhang, Y. Yayon, T. Ohta, J. L. McChesney, A. Bostwick, E. Rotenberg, K. Horn, and M. F. Crommie, Appl. Phys. Lett. **91**, 122102 (2007).
[7] Y. Zhang, V. W. Brar, F. Wang, C. Girit, Y. Yayon, M. Panlasigui, A. Zettl, and M. F. Crommie, Nat. Phys. **4**, 627 (2008).
[8] V. W. Brar, S. Wickenburg, M. Panlasigui, C.-H. Park, T. O. Wehling, Y. Zhang, R. Decker, C. Girit, A. V. Balatsky, S. G. Louie, A. Zettl, and M. F. Crommie, Phys. Rev. Lett. **104**, 036805 (2010).
[9] A. Bostwick, J. McChesney, T. Ohta, E. Rotenberg, T. Seyller, and K. Horn, Prog. Surf. Sci. **84**, 380 (2009).

[10] A. L. Vázquez de Parga, F. Calleja, B. Borca, M. C. G. Passeggi, J. J. Hinarejos, F. Guinea, and R. Miranda, Phys. Rev. Lett. **100**, 056807 (2008).
[11] B. Y. Pan, H. Zhang, D. Shi, J. Sun, S. Du, F. Liu, and H. Gao, Adv. Mater. **21**, 2777 (2009).
[12] D. Eom, D. Prezzi, K. T. Rim, H. Zhou, M. Lefenfeld, S. Xiao, C. Nuckolls, M. S. Hybertsen, T. F. Heinz, and G. W. Flynn, Nano Lett. **9**, 2844 (2009).
[13] J. Wintterlin and M. L. Bocquet, Surf. Sci. **603**, 1841 (2009).
[14] H. G. Zhang, H. Hu, Y. Pan, J. H. Mao, M. Gao, H. M. Guo, S. X. Du, T. Greber, and H.-J. Gao, J. Phys. Condens. Matter **22**, 302001 (2010).
[15] M. Gyamfi, T. Eelbo, M. Waśniowska, and R. Wiesendanger, Phys. Rev. B **83**, 153418 (2011).
[16] J. Lu, P. E. Yeo, C. K. Gan, P. Wu, and K. P. Loh, Nat. Nanotechnol. **6**, 247 (2011).
[17] B. Wang, X. Ma, M. Caffio, R. Schaub, and W.-X. Li, Nano Lett. **11**, 424 (2011).
[18] M. S. Dresselhaus and G. Dresselhaus, Adv. Phys. **51**, 1 (2002).
[19] S. Bae, H. Kim, Y. Lee, X. Xu, J.-S. Park, Y. Zheng, J. Balakrishnan, T. Lei, H. Ri Kim, Y. I. Song, Y.-J. Kim, K. S. Kim, B. Özyilmaz, J.-H. Ahn, B. H. Hong, and S. Iijima, Nat. Nanotechnol. **5**, 574 (2010).
[20] G. Giovannetti, P. A. Khomyakov, G. Brocks, V. M. Karpan, J. van den Brink, and P. J. Kelly, Phys. Rev. Lett. **101**, 026803 (2008).
[21] I. Pletikosić, M. Kralj, P. Pervan, R. Brako, J. Coraux, A. T. N'Diaye, C. Busse, and T. Michely, Phys. Rev. Lett. **102**, 056808 (2009).
[22] S. Barja, M. Garnica, J. J. Hinarejos, A. L. Vázquez de Parga, N. Martín, and R. Miranda, Chem. Commun. **46**, 8198 (2010).
[23] D. Martoccia, P. R. Willmott, T. Brugger, M. Björck, S. Günther, C. M. Schlepütz, A. Cervellino, S. A. Pauli, B. D. Patterson, S. Marchini, J. Wintterlin, W. Moritz, and T. Greber, Phys. Rev. Lett. **101**, 126102 (2008).
[24] B. Wang, M.-L. Bocquet, S. Günther, and J. Wintterlin, Phys. Rev. Lett. **101**, 099703 (2008).
[25] D. Stradi, S. Barja, C. Díaz, M. Garnica, B. Borca, J. J. Hinarejos, D. Sánchez-Portal, M. Alcamí, A. Arnau, A. L. Vázquez de Parga, R. Miranda, and F. Martín, Phys. Rev. Lett. **106**, 186102 (2011).
[26] B. Borca, S. Barja, M. Garnica, D. Sánchez-Portal, V. M. Silkin, E. V. Chulkov, C. F. Hermanns, J. J. Hinarejos, A. L. Vázquez de Parga, A. Arnau, P. M. Echenique, and R. Miranda, Phys. Rev. Lett. **105**, 036804 (2010).
[27] B. Borca, S. Barja, M. Garnica, M. Minniti, A. Politano, J. M. Rodriguez-García, J. J. Hinarejos, D. Farías, A. L. Vázquez de Parga, and R. Miranda, New J. Phys. **12**, 093018 (2010).
[28] E. Sutter, D. P. Acharya, J. T. Sadowski, and P. Sutter, Appl. Phys. Lett. **94**, 133101 (2009).
[29] C. Enderlein, Y. S. Kim, E. Rotenberg, and K. Horn, New J. Phys. **12**, 033014 (2010).
[30] H. G. Zhang and T. Greber, Phys. Rev. Lett. **105**, 219701 (2010).
[31] B. Borca, S. Barja, M. Garnica, D. Sánchez-Portal, V. M. Silkin, E. V. Chulkov, C. F. Hermanns, J. J. Hinarejos, A. L. Vázquez de Parga, A. Arnau, P. M. Echenique, and R. Miranda, Phys. Rev. Lett. **105**, 219702 (2010).
[32] S. Grimme, J. Comput. Chem. **27**, 1787 (2006).
[33] See Supplemental Material at http://link.aps.org/supplemental/10.1103/PhysRevB.85.121404 for details of the convergence of Ru(0001) electronic structure with the number of layers, the stability of the LDOS features with respect to the distance from G/Ru, and the DORS analysis in G/Ru 1x1 models using the stabilization method.
[34] G. Kresse and J. Hafner, Phys. Rev. B **47**, 558 (1993).
[35] J. P. Perdew, K. Burke, and M. Ernzerhof, Phys. Rev. Lett. **77**, 3865 (1996).
[36] G. Kresse and D. Joubert, Phys. Rev. B **59**, 1758 (1999).
[37] J. Tersoff and D. R. Hamann, Phys. Rev. Lett. **50**, 1998 (1983).
[38] F. Calleja, A. Arnau, J. J. Hinarejos, A. L. Vázquez de Parga, W. A. Hofer, P. M. Echenique, and R. Miranda, Phys. Rev. Lett. **92**, 206101 (2004).
[39] A. L. Vázquez de Parga, O. S. Hernán, R. Miranda, N. Levy Yeyati, N. Mingo, A. Martín-Rodero, and F. Flores, Phys. Rev. Lett. **80**, 357 (1998).
[40] R. M. Feenstra and J. A. Stroscio, Phys. Scr. **T19**, 55 (1987).
[41] W. A. Hofer and A. Garcia-Lekue, Phys. Rev. B **71**, 085401 (2005).
[42] By "clean reconstructed Ru" we mean the system obtained by removing the graphene layer while keeping all Ru atoms in the positions they had in the presence of graphene.
[43] B. Wang, M.-L. Bocquet, S. Günther, and J. Wintterlin, Phys. Chem. Chem. Phys. **10**, 3530 (2008).
[44] B. Wang, S. Günther, J. Wintterlin, and M.-L. Bocquet, New J. Phys. **12**, 043041 (2010).
[45] V. A. Mandelshtam, T. R. Ravuri, and H. S. Taylor, Phys. Rev. Lett. **70**, 1932 (1993).
[46] F. Martín and M. F. Politis, Surf. Sci. **356**, 247 (1996).
[47] K. Schouteden, E. Lijnen, E. Janssens, A. Ceulemans, L. F. Chibotaru, P. Lievens, and C. V. Haesendonck, New J. Phys. **10**, 043016 (2008).
[48] S. K. Hämäläinen, Z. Sun, M. P. Boneschanscher, A. Uppstu, M. Ijäs, A. Harju, D. Vanmaekelbergh, and P. Liljeroth, Phys. Rev. Lett. **107**, 236803 (2011).
[49] S. H. Phark, J. Borme, A. L. Vanegas, M. Corbetta, D. Sander, and J. Kirschner, ACS Nano**5**, 8162 (2011).
[50] D. Subramaniam, F. Libisch, Y. Li, C. Pauly, V. Geringer, R. Reiter, T. Mashoff, M. Liebmann, J. Burgdörfer, C. Busse, T. Michely, R. Mazzarello, M. Pratzer, and M. Morgenstern, Phys. Rev. Lett. **108**, 046801 (2012).
[51] N. Armbrust, J. Güdde, P. Jakob, and U. Höfer, Phys. Rev. Lett. **108**, 056801 (2012).